Journal of Applied Electrochemistry (2005) 35:715–721
DOI 10.1007/s10800-005-1400-x

Photoelectrolytic oxidation of organic species at mesoporous tungsten trioxide film electrodes under visible light illumination

R. SOLARSKA, C. SANTATO, C. JORAND-SARTORETTI, M. ULMANN and J. AUGUSTYNSKI
Département de Chimie Minérale, Analytique et Appliquée Université de Genève, 30, quai Ernest-Ansermet, CH-1211 Genève, Suisse

Received 1 July 2004; accepted in revised form 6 December 2004

Key words: mesoporous film, semiconducting WO_3, visible light photooxidation

Abstract

Operation of a photoelectrolyser fitted with a semitransparent semiconducting WO_3 film photoanode is described. Due to its band-gap energy of 2.5 eV, the photoresponse of the WO_3 electrode extends into the blue part of the visible spectrum up to 500 nm. The WO_3 photoanode exhibits particularly high incident photon-to-current efficiencies for the oxidation of several organic species with the maximum occurring at ca. 400 nm. Experiments conducted under simulated AM 1.5 solar illumination demonstrated efficient photodegradation of a variety of organic chemicals including small organic molecules as well as EDTA and anthraquinonic Acid Blue 80 dye. Although, due to the inherent mass transport limitations, the described device appears best suited to the treatment of industrial wastewater containing from 100 ppm to few g L^{-1} of impurities, almost complete removal of organic carbon was observed in several photoelectrolysis runs. This is apparently associated with the concomitant photooxidation of sulphate-based supporting electrolyte resulting in the formation of a powerful chemical oxidant-persulphate.

1. Introduction

During the late 1980s, heterogeneous photocatalysis emerged as an alternative method of hazardous waste treatment [1–7] and has already been the subject of some attempts at commercialization [7].

This technique is based principally on the use of light-harvesting TiO_2 semiconductor suspensions, which generate highly reactive positive holes at the solution interface. The oxidizing power of the positive holes is equivalent to ca. 2.6 V vs SHE in contact with neutral solutions (which is the potential of the valence band edge of TiO_2). This allows, in many cases, the total mineralization (into CO_2) of a large variety of organic compounds. The oxidative degradation of organic pollutants normally takes place in the presence of dissolved oxygen which acts, simultaneously with the positive holes, as scavenger of electrons formed in the photocatalyst. The latter process is essential in order to minimize the hole-electron recombination and thus to maintain the photocatalyst activity.

Despite having the possibility to almost totally remove low concentrations of organic substances dissolved in water, employing TiO_2 slurries as photocatalyst suffers from a series of drawbacks:

(i) the degradation process is generally considered as being too slow to be of use in commercial applications. One way to increase its rate consists in modifying the photocatalyst surface with noble metal particles to improve the kinetics of oxygen reduction. However, the latter procedure is both complex and expensive.
(ii) the use of TiO_2 slurries necessitates removal of the photocatalyst by filtration.

The above-mentioned drawbacks may be overcome by replacing the slurries by photoelectrodes, wherein an active semiconductor material is immobilized on a conducting support (such as metal or conducting glass). Furthermore, the use of a photoelectrochemical reactor configuration offers the possibility of enhancing the rate of photooxidation reactions by applying an external bias. Given that the observed photocurrents increase with light intensity, concentration of the incident light may enable photoelectrolysis to operate at even higher rates, i.e., to treat relatively concentrated solutions of pollutants.

Titanium dioxide would certainly be the ideal photocatalyst if, in addition to its excellent stability (absence of photocorrosion) over a large pH range (from pH 0 to 14) and its high photoactivity, it were also able to absorb a substantial portion of the solar spectrum. In fact, due to its absorption threshold close to 400 nm, the operation of TiO_2 photoelectrodes in solutions containing more than 20–50 ppm of contaminants requires, in practice, the use of artificial illumination sources.

This is not the case for another semiconducting oxide, WO_3, which has a band-gap energy of 2.5 eV and thus absorbs the blue part of the solar spectrum up to ca. 500 nm [8, 9]. Although the position of the conduction band of tungsten trioxide which is (slightly) too positive to allow oxygen reduction, renders the photocatalytic degradation of organic pollutants under open-circuit conditions practically impossible (C. Santato and J. Augusttynski, unpublished results) WO_3 has been shown to operate as an effective photoelectrode both under normal and concentrated solar illumination [9]. In fact, the mesoporous WO_3 photoelectrodes developed in our laboratory have demonstrated high incident-photon-to-current conversion efficiencies (IPCEs) exhibiting photocurrent doubling, reaching 190% for the photooxidation of small organic molecules [9, 10]. Importantly, the maximum in the photocurrent vs excitation wavelength spectra of the WO_3 photoelectrodes occurs at ca. 400 nm in the blue region of the solar spectrum.

Here, we show results of photoelectrolysis experiments, conducted under simulated solar AM 1.5 illumination, intended to degrade various kinds of organic chemicals in aqueous solution.

2. Experimental

The mesoporous WO_3 films used in this work were formed on conducting glass substrates by layer-by-layer deposition of a colloidal solution of tungstic acid containing an organic stabilizer and structure-directing agent – low molecular weight poly(ethylene glycol) 300. Formation of a complex between tungstic acid and the hydrophilic poly(ethylene glycol) delays the formation of fully crystallized monoclinic tungsten trioxide until ca. 500 °C. Preparation of the precursor solution has been described in detail elsewhere [11]. Conducting glass plates (Nihon Sheet Glass Co., 10 Ψ/square) consisted of a 0.5 μm thick overlayer of F-doped SnO_2. In most cases, the WO_3 films used in this work were formed by six consecutive applications of the precursor solution; each followed by annealing in flowing oxygen at 550 °C for 30 min. The final thickness of such films (determined with a Tencor Alpha Step 200 profilometer) was close to 2.5 μm. Micrographs in Figure 1, obtained with a Hitachi S-9000 scanning electron microscope, show the typical morphology of a WO_3 film after heat treatment at 550 °C. The film consists of a network of partly fused plate-like particles with sizes in the range of 2050 nm. Although annealing at 550 °C markedly develops the film porosity, it preserves the film structure, characterized by the preferential orientation of the WO_3 crystallites parallel to the substrate. As shown in Figure 1(b) the films are quite regular and smooth (their maximum protuberance has been shown to not exceed 16 nm [11]).

The photoelectrochemical measurements were carried out in a two-compartment Teflon cell equipped with a quartz window, by illuminating the WO_3 electrode either from the side of the film/solution interface or from the substrate side. The simulated solar light, AM 1.5 global, was obtained using an Oriel Model 96 000 150 W Solar Simulator fitted with a Schott 113 filter and neutral density filters. A platinum counter-electrode (large area Pt grid) was separated from the WO_3 film electrode by a Nafion membrane. In most cases the exposed surface area of the photoelectrodes was ca. 0.8 cm^2. The potential of the WO_3 electrode was monitored vs a saturated calomel reference electrode and is quoted vs reversible hydrogen electrode (RHE) in the same solution. A Princeton Applied Research Model 362 scanning potentiostat was used in the electrochemical measurements. The CO_2 content in the effluent gas from the photoelectrolysis cell was determined on a Hewlett Packard 5890 Series II gas chromatograph equipped with a TCD detector and the Carbosieve S-II column.

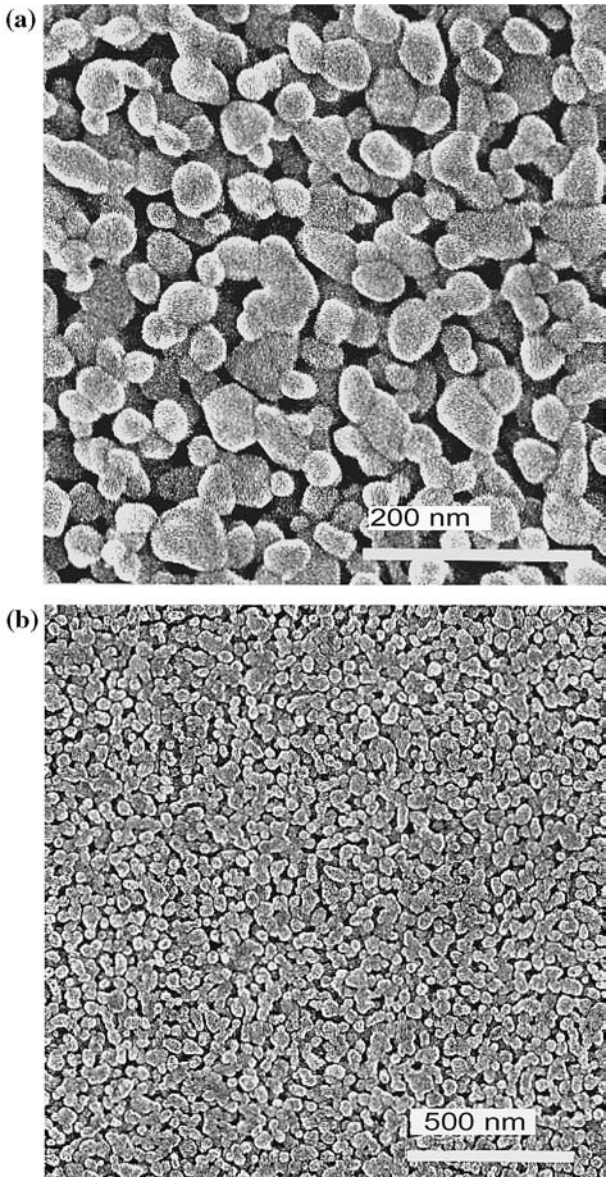

Fig. 1. Scanning electron micrographs showing surface views of a mesoporous WO_3 film. Bars are 200 nm for (a) and 500 nm for (b).

UV–Vis spectra were recorded on a Perkin–Elmer Lambda 900 spectrophotometer. Acid Blue 80 (dye content ca. 60%) was obtained from Aldrich. All other reagents were analytical grade.

Degradation of ethylenediaminetetraacetic acid (EDTA) occurring during photoelectrolysis runs was monitored by high performance liquid chromatography (HPLC) using the method described by Bergers and De Groot [12]. Shortly, EDTA was chelated with an excess of $FeCl_3$ forming a Fe^{3+}/EDTA complex having a high stability constant. Separation was performed using reversed-phase ion-pair liquid chromatography followed by UV absorbance detection of the iron complex at 254 nm. Formation of formaldehyde was followed using the chromotropic method.

3. Results and discussion

3.1. *Steady-state photocurrent-potential characteristics of WO_3 photoelectrodes*

Unlike nanoparticulate TiO_2 photoelectrodes, at which the photooxidation of water is almost suppressed [13], WO_3 photoelectrodes exhibit high activity both in acidic inorganic solutions and in the presence of various organic species. Figure 2(a) shows photocurrent–voltage curves for a WO_3 film electrode, irradiated with simulated solar AM 1.5 light, measured in 3 M $H_2SO_{4(aq)}$ solution and after addition of 0.1 mol L^{-1} of CH_3OH. Despite the fact that WO_3 absorbs only the blue part of the solar spectrum, the saturation photocurrents recorded in the solution of sulphuric acid exceed 4 mA cm^{-2} and those corresponding to the photooxidation of methanol, 8 mA cm^{-2}. In the case of the latter, the large increase of the photocurrent, which is also observed in the presence of other small organic molecules (*vide infra*), is illustrative of photocurrent doubling [14, 15] occurring efficiently at the WO_3 electrode [9, 10]. This is supported by the fact that the IPCEs determined for the oxidation of small organic molecules, exemplified by those recorded in methanol solution depicted in Figure 2(b), markedly exceed 100% over a broad region of the photocurrent spectrum (from 300 to 450 nm). However, as shown in Figure 2(a), in the initial part of the I_{ph}-E curve, the photocurrents recorded in the presence of methanol are clearly more than twice as large as those obtained in the supporting electrolyte alone. The latter observation, together with the negative shift of the onset potential visible in Figure 2(a), clearly confirm that a relatively concentrated 0.1 M methanol solution undergoes preferential photooxidation at the WO_3 photoanode, independent of the occurrence of the photocurrent doubling. Spectroscopic evidence [16] suggests that under the latter conditions the photooxidation process is initiated by the direct hole transfer to adsorbed alcoholic species rather than by the reaction with photogenerated hydroxyl radicals:

$$h^+_{vb} + CH_3OH_{ad} \rightarrow^{\bullet} CH_2OH_{ad} + H^+$$

followed by electron injection into the conduction band of the semiconductor by the $^{\bullet}CH_2OH_{ad}$ radical:

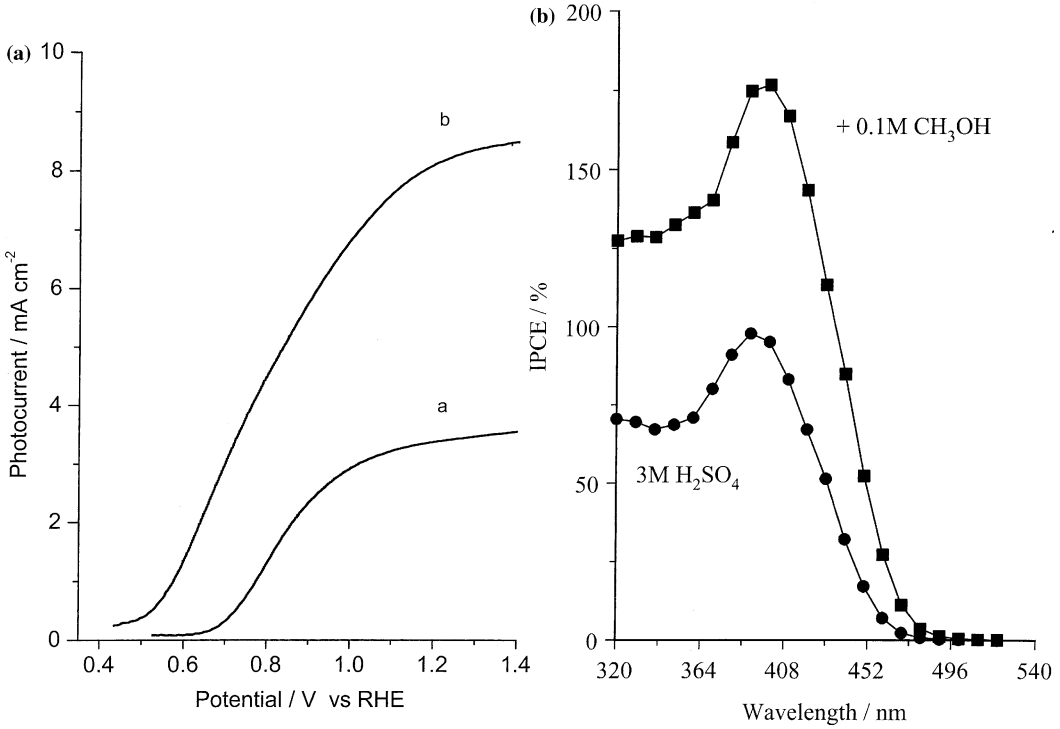

Fig. 2. (a) Typical photocurrent-potential plots for a ca. 2.5 μm thick WO_3 film electrode, illuminated with simulated AM 1.5 solar light. Photocurrent-potential plots recorded in 3 M $H_2SO_{4(aq)}$ (curve a) and after addition of 0.1 mol l^{-1} of methanol (curve b); (b) The corresponding photocurrent vs wavelength spectra.

$$^{\bullet}CH_2OH_{ad} \rightarrow CH_2O + H^+ + e^-_{cb}$$

However, the indirect oxidation pathway is likely to prevail at lower methanol concentrations, at which the observed photocurrents strongly decrease (cf. Figure 3). One possible explanation is the concomitant decrease in coverage of the WO_3 electrode by adsorbed CH_3OH molecules, which also results in a less effective doubling of the photocurrent. It should be recalled that photoelectrolyses of sulphate based electrolytes revealed the formation of substantial amounts of persulphate species, with the current efficiencies exceeding 80% for 3 M $H_2SO_{4(aq)}$ and reaching ca. 15% in a 0.1 M Na_2SO_4 solution. The formation of the $S_2O_8^{2-}$ species in the electrolyte was monitored by means of Raman spectroscopy by comparing intensity of the bands at 840 and 1080 cm^{-1} with those at 981 and 1051 cm^{-1} corresponding to the SO_4^{2-} and HSO_4^- ions [17].

Thus, prior to the persulphate species, the photogenerated $SO_4^{\bullet}$ radicals appear as plausible intermediates in the oxidation of dilute solutions of organic species containing sulphate ions as a part of the supporting electrolyte:

$$SO_4^{\bullet -} + CH_3OH \rightarrow {}^{\bullet}CH_2OH + HSO_4^-$$

$$SO_4^{\bullet -} + {}^{\bullet}CH_2OH \rightarrow CH_2O + HSO_4^-$$

Total oxidation of methanol to form CO_2 involves the transfer of six electrons and formation of formaldehyde and formic acid intermediate species. As shown in Figure 4, all of them exhibit comparable, high photooxidation rates at the WO_3 photoanode and a similar extent of photocurrent doubling.

3.2. *Photoelectrochemical degradation of organic chemicals*

In order to evaluate the practical ability of the photoelectrochemical cell to degrade organic chemicals, 30 cm^3 quotas of solutions of a series of organic compounds (including, in particular, methanol, formaldehyde and formic acid) were electrolyzed at a 0.8 cm^2 WO_3 photoanode illuminated with simulated solar (AM 1.5) light, the platinum counter electrode was placed in a second compartment and separated with a Nafion membrane. Due to their diverse uses these compounds are frequently present in industrial effluents from which they have to be removed in order to avoid damage to aquatic environment.

Prolonged photoelectrolyses of 0.01 M solutions of CH_3OH, HCOOH and CH_2O with 0.1 M $NaHSO_4$ as supporting electrolyte, demonstrated the ability of the WO_3 electrodes to perform a practically complete mineralization of the organic species, despite the diffusion limitations, with the total organic carbon content, TOC, reaching ca. 3 ppm. This result is consistent with both $SO_4^{\bullet}$ radicals and $S_2O_8^{2-}$ ions acting as oxidising species at the final stages of the photoelectrolysis.

The occurrence of the 3-step methanol oxidation (involving first formation of formaldehyde and then that

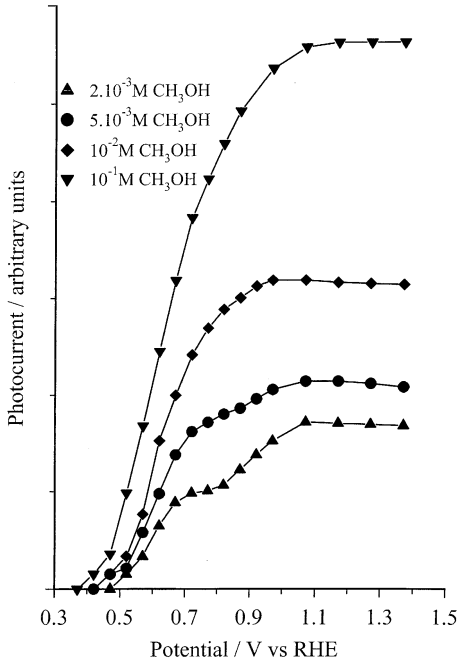

Fig. 3. Effect of the methanol concentration upon relative amount of the photocurrent recorded at a WO_3 film electrode under 1 sun AM 1.5 illumination. 1 M $NaHSO_{4(aq)}$ (pH 2) was used as a supporting electrolyte.

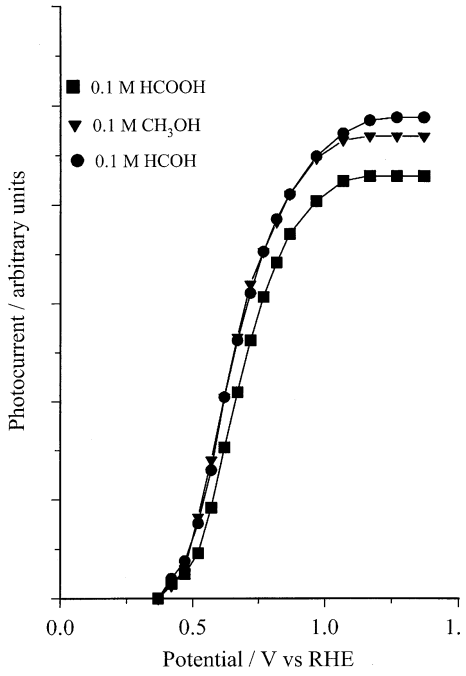

Fig. 4. Comparison of photocurrent-potential plots recorded at a WO_3 film electrode in the presence of 0.1 mol L^{-1} of, respectively, methanol. formaldehyde and formic acid. 1 M $NaHSO_{4(aq)}$ (pH 2) served as supporting electrolyte. Simulated AM 1.5 solar light illumination.

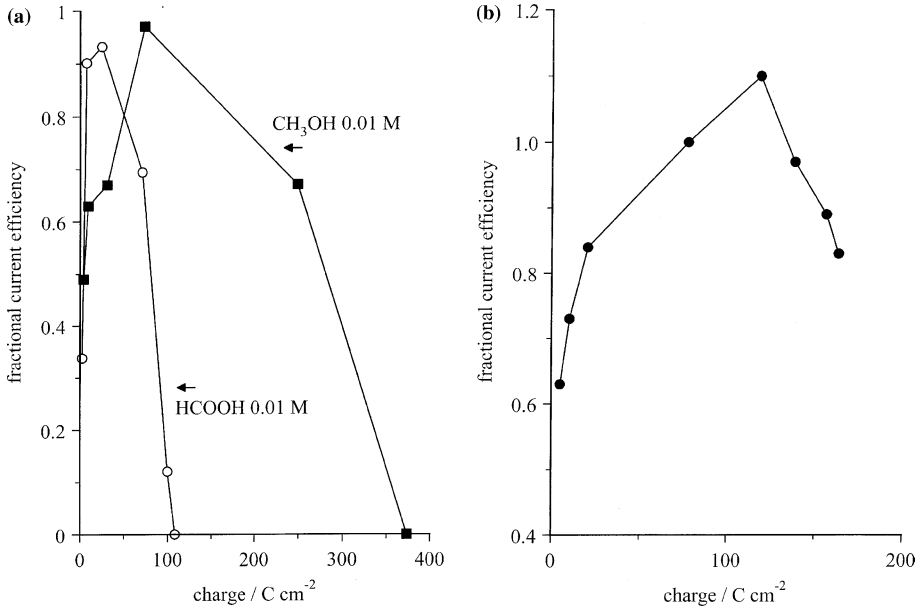

Fig. 5. Changes in the current efficiency observed during prolonged photoelectrolysis of 30 ml of 10^{-2} M solutions of (a) formic acid and methanol and (b) oxalic acid at a WO_3 film electrode under 1 sun AM 1.5 illumination. 1 M $NaHSO_{4(aq}$ (pH 2) was the supporting electrolyte. Applied bias voltage 1 V. The current yields were derived from the amount of formed CO_2 and are plotted against the amount of electric charge.

of formic acid) is confirmed by the instantaneous current efficiencies for CO_2 formation shown in Figure 5(a) The efficiency for the oxidation of methanol is progressively rising from an initial value of 50% to about 100%. In the case of formaldehyde (not shown) and formic acid, the efficiencies increased more rapidly to reach almost 100%. Despite a low residual concentration level of the organic species attained during these photoelectrolyses, the mean current efficiencies remained close to 80%. Similar high current efficiencies were also observed during photoelectrolysis of another small organic molecule – oxalic acid. The fact that in the latter case the amount of formed CO_2 exceeded that expected from a photoelectrochemical (faradaic) process (cf. Figure 5(b)) may suggest a simultaneous occurrence of a homogeneous photochemical reaction in the solution.

Figure 6 shows results of the photoelectrochemical degradation of EDTA (ethylenediaminetetraacetic acid). This chemical is used in various branches of the industry (textile, paper, pharmacy, photography, nuclear plants), and is also present in detergents. Because EDTA is not volatile, it is largely released in waste water. It is to be noted that EDTA is neither transformed by microorganisms nor adsorbed in the sewage sludge. One form, the Fe(III)–EDTA, complex, undergoes direct photolysis, but this process produces toxic formaldehyde [18]. At the pH of the supporting electrolyte used in this experiment, the essentially undissociated EDTA undergoes preferential photooxidation at the WO_3 with respect to the reaction intermediate-formaldehyde. This is consistent with the progressive build-up of the CH_2O concentration during the first part of the photoelectrolysis, accompanying decrease of the amount of EDTA (cf. Figure 6). It is only after virtual disappearance of the EDTA from the solution that the photooxidation of formaldehyde becomes in turn the main reaction at the WO_3 electrode.

Another important class of harmful chemicals discharged in significant volumes into water treatment plants, where they are usually transformed into sludge, are azo dyes. Due to their mesoporous structure, wherein the solution fills the pores down to the substrate, the WO_3 film electrodes are especially well suited for the photoelectrolytic oxidation of intensely

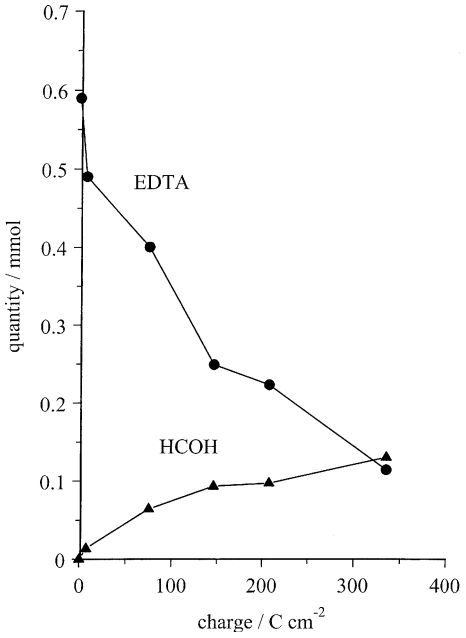

Fig. 6. Degradation of EDTA and concomitant formation of formaldehyde at a WO_3 film electrode, illuminated with 1 sun AM 1.5, plotted as a function of electric charge. Photoelectrolysis was conducted in a 10^{-2} M EDTA/1 M H_2SO_4 aqueous solution (60 ml) under the applied bias of 0.8 V.

colored dyes solutions. In fact, the possibility to operate under back side (i.e., through the substrate) WO_3 film illumination limits to a large extent the absorption losses due to the dye solution. However, the optical losses associated with the transmission of the visible light through the conducting glass are not negligible, 30% on an average. In spite of this, the WO_3 film electrode, illuminated from the back side with simulated solar AM 1.5 light, operated in intensely blue colored solution of an anthraquinonic dye Acid Blue 80 at current densities larger than 2 mA cm^{-2}. Photocatalytic degradation of the latter dye on dispersed TiO_2 P25 nanoparticles, illuminated with high intensity xenon and/or mercury lamps, has recently been described by Augugliaro and coworkers [19].

In Figure 7 are shown UV–visible absorption spectra of an aqueous solution comprising 30 ppm of the dye taken at different time intervals of the photoelectrolysis.About 45 ml of the dye solution contained in the cell, bubbled slowly with nitrogen, was oxidized at a 0.8 cm^2 WO_3 photoanode polarized at 1 V with respect to the H_2-evolving Pt cathode placed in a separated compartment of the cell, filled with the supporting electrolyte (0.1 M $NaHSO_{4(aq)}$, pH 2). Instantaneous Faradaic efficiences based on the CO_2 content in the effluent gas are plotted in Figure 8. Accordingly, at this stage of photoelectrolysis, about 70% the electric charge was used to form reaction intermediates (including NO_3^- and SO_4^{-2} ions originating from the dye) and possibly also persulphate species and oxygen. Importantly, as indicated by a moderate decrease in the photocurrent, the mesoporous WO_3 film remained stable and active along the whole photoelectrolysis run.

3.2.1. *Photoelectrolytic degradation vs conventional electrolytic treatment of wastewater*

Clearly, a cheap and efficient method suitable for degradation of organic pollutants present in the amounts of 1–10 g L^{-1} of solution is presently lacking. The use of TiO_2 as a photocatalyst or as an electrode material in photoelectrochemical cells represents a possible option but involves large energy consumption associated with the necessity of artificial UV illumination. On the other hand, a large number of organic compounds present in the effluents are refractory to a conventional electrolytic treatment [20]. This is, for example, the case for formic, oxalic or maleic acids which all undergo easy photooxidation at the WO_3. The photoelectrolytic cell using a WO_3 film electrode can operate under solar light illumination and requires only a small fraction of the electrical energy needed by a conventional electrolytic oxidation. This is due both to a much lower voltage at which the photoelectrolytic device operates and to a much larger portion of the current used directly to oxidize organic substances. In fact, while the conventional electrochemical oxidation of most of organic compounds requires high-oxygen-overvoltage anodes (consisting of PbO_2 or doped SnO_2-coated titanium [20, 21] or of carbon derived materials [22]) and, consequently, large cell voltages on the order of 4–5 V, the WO_3 photoanodes using solar light as a part of energetic input can operate under a five times lower bias, i.e., 0.8–1 V. In addition, most of the organic compounds undergo preferential photooxidation (with respect to water) at the WO_3 photoanode, which is in contrast with their electrochemical oxidation often exhibiting low current efficiencies. Even assuming that the mean current efficiency associated with the photoelectrolysis is only two times higher than that of the corresponding electrolysis, the specific energy requirement for this new process may be even ten times lower than that for the conventional one. Thus, the energy requirement for the removal from the waste stream of the amount of organics equivalent to 1 kg of COD (chemical oxygen demand) would be only on the order of 5 kWh instead of 30–50 kWh estimated for the electrochemical oxidation [20].

4. Conclusions

The described photoelectrochemical cell equipped with a semitransparent WO_3 electrode exhibits a series of unique features:

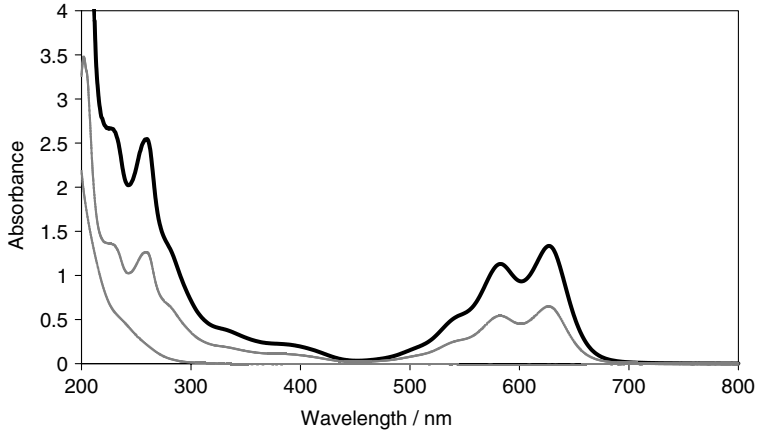

Fig. 7. Changes in the absorbance of an Acid Blue dye solution (initial concentration 30 ppm) recorded at different stages of photoelectrolysis at a WO_3 film electrode conducted under 1 sun AM 1.5 illumination. Applied bias voltage 1 V.

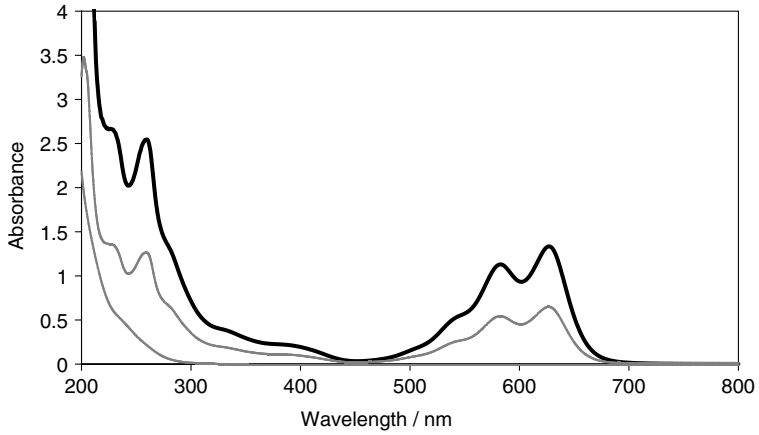

Fig. 8. Evolution of the current yield of CO_2 formation during photoelectrolysis of an Acid Blue 80 dye solution (initial concentration 30 ppm), conducted at a WO_3 film electrode under 1 sun AM 1.5 illumination. 0.1 M $NaHSO_{4(aq)}$ (pH 2) was the supporting electrolyte. Applied bias voltage 1 V.

(i) Large photocurrents generated under AM 1.5 solar light illumination in spite of the absorption range of the WO_3 film restricted to the blue part of the spectrum (up to 500 nm). This is principally due to high quantum efficiencies for the photooxidation of organic species.
(ii) Excellent stability (absence of photocorrosion) in both moderately and highly acidic solutions.
(iii) Formation of a chemical oxidant-persulphate species in a parallel reaction occurring at the photoanode in sulphate based supporting electrolytes. This reaction is expected to play an increasing role with decreasing the concentration of organic hole scavengers.

The observed photocurrents for the oxidation of organic species under 1 sun illumination are in fact close to the mass transport limited currents in the presence of ca 1 g L^{-1} of organic chemicals in the solution. However, more concentrated effluents can be treated under moderately concentrated solar light.

Acknowledgements

This work was supported by the Swiss National Science Foundation and the Swiss Federal Office of Energy.

References

1 M. Schiavello (Ed.), 'Photocatalysis and Environment: Trends and Applications', NATO ASI Series, Vol. C237 (Kluwer Academic, Dordrecht, The Netherlands, 1988).
2. N. Serpone and E. Pelizzetti, Photocatalysis: Fundamentals and ApplicationsWiley-InterscienceNew York.
3. C. Guillard, J.M. Herrmann and P. Pichat, *Catal. Today* **17** (1993) 7.
4. D.F. Ollis and H.A. Al-Ekabi, Proceedings of the 1st International Conference on TiO_2 Photocatalytic Purification and Treatment of Water and AirElsevierAmsterdam.
5. D.W. Bahnemann, J. Cunningham, M.A. Fox, E. Pelizzetti, P. Pichat and N. Serpone, 'Aquatic Surface Photochemistry' (F.L. Lewis, Boca Raton. FL, 1994) p. 261.
6. K. Rajeshwar, *J. Appl. Electrochem.* **25** (1995) 1067.
7. D.M. Blake, 'Bibliography of Work on the Heterogeneous Photocatalytic Removal of Hazardous Compounds from Water and Air', NREL/TP-510-31319 (National Renewable Energy Laboratory, Golden, CO, 2001).
8. M. Spichiger-Ulmann and J. Augustynski, *J. Appl. Phys.* **54** (1983) 6061.
9. C. Santato, M. Ulmann and J. Augustynski, *J. Phys. Chem. B* **105** (2001) 936.
10. C. Santato, M. Ulmann and J. Augustynski, *Adv. Mater.* **13** (2001) 511.
11. C. Santato, M. Odziemkowski, M. Ulmann and J. Augustynski, *J. Am. Chem. Soc.* **123** (2001) 10639.
12. P.J.M. Bergers and A.C. GrootDe, *Water Res.* **28** (1994) 639.
13. A. Wahl, M. Ulmann, A. Carroy and J. Augustynski, *J. Chem. Soc., Chem. Commun.* (1994) 2277.
14. S.R. Morrison and T. Freund, *J. Chem. Phys.* **47** (1967) 1543.
15. T. Freund and WP. Gomes, *Catal. Rev.* **3** (1969) 1.
16. A. Léausic, F. Babonneau and J. Livage, *J. Phys. Chem.* **90** (1986) 4193.
17. C. Santato, H. Hagemann and J. Augustynski, to be published.
18. F.G. Kari, S. Hilger and S. Canonica, *Environ. Sci. Technol.* **29** (1995) 1008.
19. A.B. Prevot, C. Baiocchi, M.C. Brussino, E. Pramuaro, P. Savarino, V. Augugliaro, G. Marci and L. Palmisano, *Environ. Sci. Technol.* **35** (2001) 971.
20. S. Stucki, R. Kötz, B. Carcer and W. Suter, *J. Appl. Electrochem.* **21** (1991) 99.
21. C.L.P.S. Zanta, P.-A. Michaud, Ch. Comninellis, A.R. Andradede and J.F.C. Boodts, *J. Appl. Electrochem.* **33** (2003) 1211.
22. A.M. Polcaro and S. Palmas, *Ind. Eng. Chem. Res.* **36** (1997) 1791.